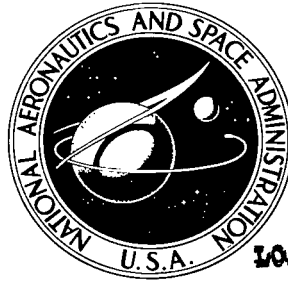


NASA TECHNICAL NOTE



NASA TN D-5603

c.1

LOAN COPY: RETURN TO
AFWL (WLOL)
KIRTLAND AFB, N MEX

0132572



NASA TN D-5603

EXPERIMENTAL EVALUATION OF
VOLT-AMPERE LOADING AND OUTPUT
DISTORTION FOR A TURBOALTERNATOR
WITH MULTIPLE LOAD PHASE-CONTROLLED
PARASITIC SPEED CONTROLLER

by Dennis A. Perz and Martin E. Valgora

*Lewis Research Center
Cleveland, Ohio*



0132572

1. Report No. NASA TN D-5603	2. Government Accession No.	3. Recipient's Catalog No.	
4. Title and Subtitle EXPERIMENTAL EVALUATION OF VOLT-AMPERE LOADING AND OUTPUT DISTORTION FOR A TURBOALTERNATOR WITH MULTIPLE LOAD PHASE-CONTROLLED PARASITIC SPEED CONTROLLER		5. Report Date December 1969	
		6. Performing Organization Code	
7. Author(s) Dennis A. Perz and Martin E. Valgora		8. Performing Organization Report No. E-5136	
		10. Work Unit No. 120-27	
9. Performing Organization Name and Address Lewis Research Center National Aeronautics and Space Administration Cleveland, Ohio 44135		11. Contract or Grant No.	
		13. Type of Report and Period Covered Technical Note	
12. Sponsoring Agency Name and Address National Aeronautics and Space Administration Washington, D. C. 20546		14. Sponsoring Agency Code	
		15. Supplementary Notes	
16. Abstract The reduction of alternator volt-ampere loading and output distortion by means of multiple phase-controlled parasitic loads is evaluated. Experimental data are compared with an analysis made previously. Results show that test circuit reactances greatly reduce the expected level of current distortion. Current distortion is significantly reduced by using two parasitic loads instead of one but little further reduction occurs for three loads. This results from design limitations in the parasitic load phase control circuitry. Experimental data for volt-ampere loading agrees well with predictions.			
17. Key Words (Suggested by Author(s)) Turboalternator systems Speed controllers Energy conversion systems		18. Distribution Statement Unclassified - unlimited	
19. Security Classif. (of this report) Unclassified	20. Security Classif. (of this page) Unclassified	21. No. of Pages 35	22. Price * \$3.00

*For sale by the Clearinghouse for Federal Scientific and Technical Information
Springfield, Virginia 22151



CONTENTS

	Page
SUMMARY	1
INTRODUCTION	2
DESCRIPTION OF PARASITIC TYPE SPEED CONTROLLERS	3
Parasitic Loading and Phase Control	3
Ideal Model and Experimental System	4
EXPERIMENTAL APPARATUS	6
Description of Developmental Components	6
Description of Auxiliary Test Equipment	7
RESULTS AND DISCUSSION	8
Waveform Analysis	8
Current Distortion	13
Voltage Distortion and Crest Factor	17
Volt-Ampere Requirements	19
SUMMARY OF RESULTS	26
APPENDIXES	
A - SYMBOLS	27
B - INSTRUMENT SPECIFICATIONS	29
C - CALCULATION OF 1 PER UNIT PARASITIC LOAD VALUES FROM EXPERIMENTAL DATA	31
REFERENCES	33

EXPERIMENTAL EVALUATION OF VOLT-AMPERE LOADING AND OUTPUT
DISTORTION FOR A TURBOALTERNATOR WITH MULTIPLE LOAD
PHASE-CONTROLLED PARASITIC SPEED CONTROLLER

by Dennis A. Perz and Martin E. Valgora

Lewis Research Center

SUMMARY

An evaluation of the experimental effects of multiple phase-controlled parasitic loads on turboalternator output is presented. Phase-controlled loading introduces unwanted effects in an electrical system. These effects include an increase in alternator volt-ampere (apparent power) loading. In addition, substantial current and voltage harmonics are generated. One means of reducing these effects is through the use of multiple parasitic loads which are sequentially activated. An analysis of phase-controlled loading and the operation of multiple parasitic loads has been made previously.

As a means of comparison, this report presents experimental results obtained from testing a 400-hertz Brayton cycle turboalternator and its associated controls. Harmonic distortion and volt-ampere loading are analyzed as functions of parasitic load. The number of parasitic loads and the useful load power factor are used as parameters.

Comparisons indicate that current harmonics in experimental systems are generally lower than predicted previously. This results from the effects of experimental test circuit reactances not considered in the prior analysis.

Division of the parasitic load into two sections produces significant reduction in current distortion as predicted. Increasing the number of parasitic loads beyond two, however, results in only a slight further reduction in alternator current distortion. This occurs because of design limitations in the speed controller related to the maximum attainable conduction interval of the phase-controlled switch. In general, the greater the attainable conduction interval, the more the distortion can be reduced.

The measured increase in alternator volt-ampere rating necessitated by operation of one, two, or three parasitic loads was in each case within 1 percent of the predicted values.

INTRODUCTION

Turboalternator speed can be controlled by adjusting either turbine input or alternator output. Adjustment of alternator load by static phase-controlled switches, herein termed parasitic loading, is attractive for dynamic power conversion systems having fixed input sources. Systems currently under investigation for space applications using the Brayton thermodynamic cycle are typical (refs. 1 and 2). The parasitic load operates in parallel with the system useful load and compensates for variations in the useful load such that the total alternator load remains constant. With fixed turbine input power, no other means of turbine speed regulation is necessary. With parasitic loading, all thermal and rotating components operate continuously at a single design point independent of the useful load output.

Phase control is an operation by which electric current can be made to conduct over any desired fraction of a half cycle of a sine wave. Other types of parasitic loading are possible using Prony brakes or variable transformers, but phase control offers the advantages of fast response, continuous accurate power adjustments, static operation, and high reliability.

Phase-controlled loading does, however, introduce some undesirable effects in an electrical system. In particular, an increase in the volt-ampere rating of the turboalternator is necessitated as noted in the case of the SNAP-8 alternator discussed in reference 3. Also, significant harmonic distortion is introduced in the electrical output. One means of reducing these effects is through the use of multiple, sequentially operated parasitic loads. The use of multiple loads has the effect of minimizing the magnitude of the phase-controlled component of the total current. A multiple parasitic load configuration has been used previously in the development of the SNAP-2 power system (ref. 4). In addition, Gilbert has analyzed the effects of multiple parasitic loads in reference 5.

This report presents experimental results of a test program carried out on a 400-hertz Brayton cycle turboalternator and controls currently being evaluated by NASA (ref. 6). The turboalternator and associated voltage regulator-exciter were designed and fabricated under contract NAS 3-6013 by Pratt & Whitney Aircraft and the General Electric Company (ref. 7). The parasitic speed controller tested was designed and built at the Lewis Research Center.

The primary purpose of this report is to make an experimental evaluation of the effects of multiple phase-controlled parasitic loads on a turboalternator electrical system. The variations of volt-ampere loading, current and voltage distortion, and voltage crest factor with parasitic loading are discussed. The analysis of experimental results is directed, as much as possible, toward a generalized presentation of real systems rather than as simply the operating characteristics of the Brayton cycle system tested.

In this way certain general conclusions, applicable to any turboalternator system using phase-controlled parasitic loading, can be made. In addition, a comparison of experimental results with the theoretical analysis of reference 5 is made to determine the accuracy and limitations of that analysis. For the purposes of comparison, several figures and curves originally published in reference 5 are reproduced herein. In all cases they are labelled "theoretical."

DESCRIPTION OF PARASITIC TYPE SPEED CONTROLLERS

Parasitic Loading and Phase Control

A simplified block diagram of a parasitically loaded turboalternator is shown in figure 1. Alternator output is absorbed by two distinct loads. The first of these is the

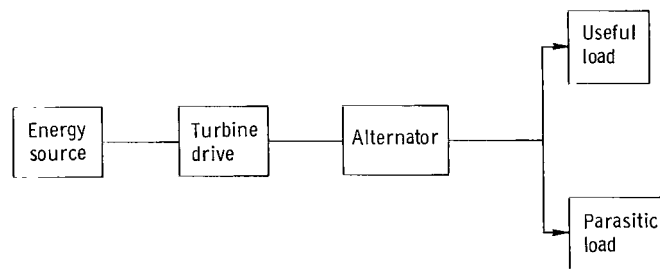


Figure 1. - Turboalternator with parasitic load.

useful load, which consists of all systems and equipment designated as part of an assigned mission. This includes auxiliary turboalternator controls such as the voltage regulator-exciter. The remainder of the alternator output is absorbed by the parasitic load, which acts primarily to compensate for variations in the useful load and thereby keeps the total alternator loading constant. The parasitic load consists of a speed controller for power variation and resistors for power dissipation.

The amount of parasitic load applied to the alternator depends on turbine speed (which is equivalent to alternator electrical frequency). When the turboalternator speed has reached steady state, any variation in the useful load results in a change in the torque load on the turbine. As a result, shaft speed also changes because turbine input power remains constant. This change is sensed by the speed controller which then adjusts the parasitic load to offset the change in useful load. The sensitivity or gain of the speed controller is high enough to yield satisfactory speed and frequency regulation.

Adjustment of power in the parasitic load is accomplished through phase-controlled operation of static switching devices. Phase control is an operation by which an electric switching device can be made to begin conducting current at any desired "firing" angle α ($0^\circ \leq \alpha \leq 180^\circ$) in a half cycle of a sine wave. Control of this firing angle yields control of the effective current into the parasitic resistor and thus control of parasitic power.

Phase-controlled currents are periodic but nonsinusoidal. This latter characteristic is the source of harmonic distortion in the alternator output. In addition, the fundamental component of the phase-controlled current lags the applied voltage (see appendix B in ref. 5), thereby increasing the alternator volt-ampere loading over that created by a purely resistive load.

In order to minimize the output distortion and volt-ampere loading effects created by phase control operation and yet maintain this type of control, the parasitic load can be broken down into multiple, sequentially operated loads. The purpose is to minimize at all times the size of the phase-controlled currents and, therefore, the adverse effects produced.

The analysis of the effects of multiple parasitic loads on distortion and volt-ampere loading is twofold in approach in this report. First, an experimental evaluation of these effects is made as a result of testing a real system. This evaluation is then compared with results from the theoretical analysis in reference 5. To facilitate these objectives, brief descriptions of the makeup and operation of the ideal model (from ref. 5) and the experimental test system are presented. Discussion of the latter is kept general because the system tested is considered representative of several currently under development.

Ideal Model and Experimental System

Figure 2 is a schematic diagram of a turboalternator electrical system with multiple

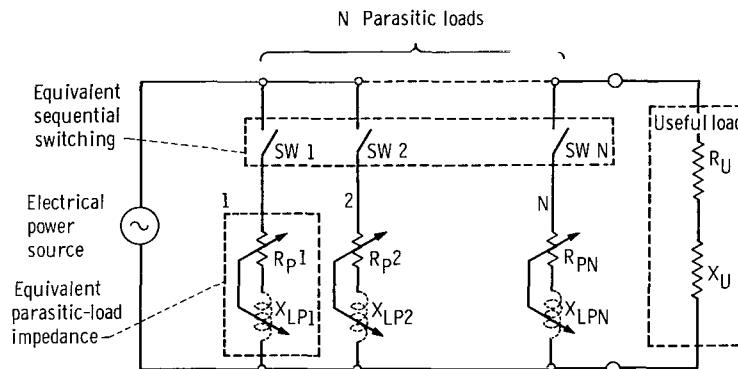


Figure 2. - Schematic diagram of theoretical ac voltage source with multiple parasitic loads.

parasitic loads. The voltage source is assumed ideal, having a zero internal impedance and a constant amplitude, zero distortion output. The useful load is assumed to consist of linear resistances and reactances.

The N parallel parasitic loads are simulated by the sequential switching and the impedance $R_{PK} + X_{LPK}$. (Symbols are defined in appendix A.) Although the loading element is purely resistive, X_{LPK} (which is equivalent to X_{LP} in ref. 5) is shown as an equivalent inductive reactance, which is characteristic of phase-controlled operation. The impedance is nonlinear and variable with the firing angle α . It should be noted that a linear load is one whose impedance is constant with variations in time and voltage and which, therefore, does not introduce any harmonic distortion into the current passing through it.

In the ideal model, only one parasitic load is adjusted at a time. Each is variable over the conduction interval $0^\circ \leq \alpha \leq 180^\circ$ for every half cycle of the applied voltage. As frequency increases from a minimum, the first parasitic load begins to turn on and absorb power. As the frequency continues to increase, the power dissipated increases until 180° conduction per half cycle occurs. If additional parasitic power is necessary, the second load begins to turn on. This process continues until all parasitic loads are turned fully on at which time the full alternator output is absorbed by the parasitic loads. Note that ideally a phase-controlled current conducting for 180° per half cycle is a sinusoid with zero distortion and represents a purely resistive load. Thus the only distortion in the system is produced by that parasitic load which is partially turned on.

In figure 3 a simplified equivalent circuit of the experimental test setup is shown. The voltage source is an alternator with equivalent internal impedance $R_A + X_A$. The internally generated voltage is E_G and the terminal voltage is E_T . The impedance of

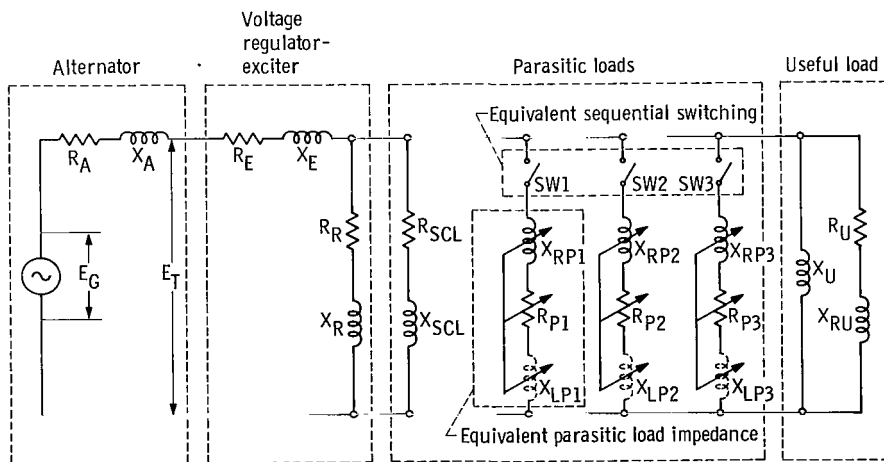


Figure 3. - Schematic diagram of experimental test circuit using three parasitic loads.

the voltage regulator-exciter is shown separately from the useful load because of the location of the series impedance $R_E + X_E$. This is actually a transformer winding which is part of the static exciter. The equivalent shunt impedance of the regulator circuitry is $R_R + X_R$.

The load produced by the parasitic control circuitry is represented by $R_{SCL} + X_{SCL}$. In the case of minimum parasitic load, this impedance represents the shutoff losses. The equivalent impedance of the parasitic loads is represented by the sequential switching and by the sum of $X_{RPK} + R_{PK} + X_{LPK}$ for each of the loads. The subscript K indicates the specific parasitic load. The reactance of autotransformers in the parasitic load bank, which is used to simulate the parasitic resistors, is represented by X_{RPK} . These autotransformers are provided to give continuous adjustment of the effective value of R_{PK} in the experimental test circuit. Again, the equivalent parasitic load impedance is shown to be variable as a result of the nonsinusoidal phase-controlled currents.

The application of parasitic load in experimental systems differs from that assumed in the ideal model in that overlap is built into the frequency sensing circuits; that is, before the first parasitic load is fully on, the second has already begun to turn on. This overlap is necessitated in order to produce a reasonably smooth loading characteristic (parasitic power as a function of frequency).

The parallel combination of R_U and X_U is the equivalent of the useful load impedance as connected in the experimental test circuit. As before, X_{RU} is a load bank autotransformer.

EXPERIMENTAL APPARATUS

Description of Developmental Components

Figure 4 is a simplified block diagram of the experimental test circuit used which shows both test hardware and instrumentation. The turboalternator is a 12 000 rpm machine which operates on gas lubricated bearings. The alternator is a brushless, three-phase, 400-hertz, homopolar inductor. At design turbine inlet conditions the electrical output is approximately 9 kilowatts at 0.8 lagging power factor. The voltage regulator-exciter functions to supply excitation to the alternator field and acts to regulate the voltage at the useful load.

The parasitic speed controller uses silicon controlled rectifiers (SCR's) for power variation. The SCR's are used because of their low shutoff losses occurring when the parasitic load is at a minimum. Because SCR's conduct current in only one direction, they automatically turn off at the end of each half cycle of operation. When they are used in parallel pairs, one conducting in each direction, the result is bidirectional power control.

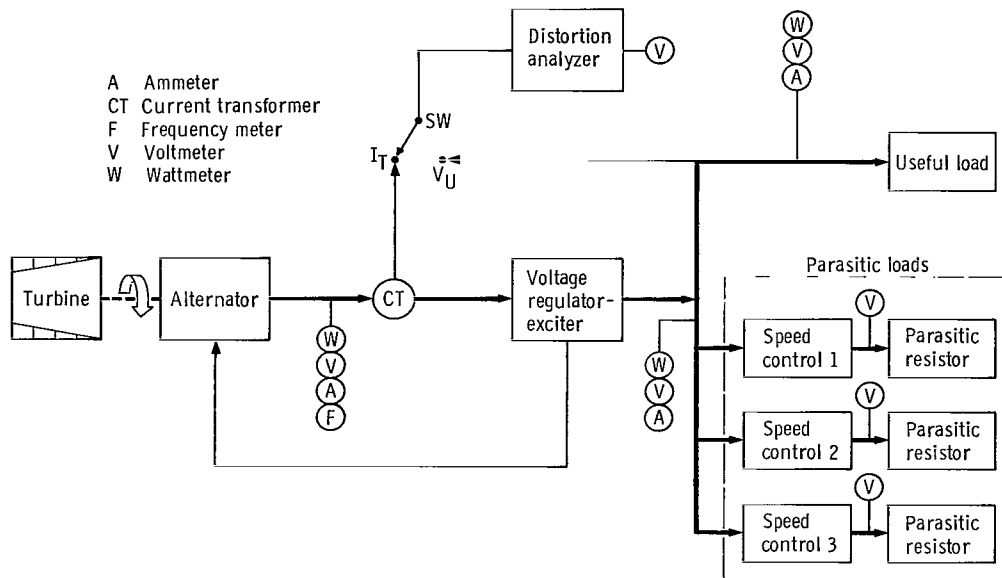


Figure 4. - Block diagram of electrical test setup.

The breadboard speed controller tested consists of 3 three-phase parasitic loads. The speed controller is designed to have a total capacity of 180 percent (16.2 kW) of the nominal turboalternator output power (9 kW). This overrating is introduced to improve dynamic response and to provide redundancy. During normal steady-state operation, only the first parasitic load plus part of the second is ever loaded. For the purposes of this testing, however, this overrating is not applied. The speed controller is tested in configurations using one, two, or three parasitic loads. In each case the sum of all parasitic loads fully on equals the nominal turboalternator rating of 9 kilowatts. Thus, the results of this report should not be interpreted as representing the operation of this Brayton system under "design" conditions.

Detailed descriptions of the hardware used plus individual experimental test characteristics can be found in references 8 to 11.

Description of Auxiliary Test Equipment

The useful load and the parasitic resistors shown in figure 4 are simulated by commercial load banks consisting of essentially linear resistors and inductors. The useful load bank is adjustable and is capable of providing power factors from unity to zero lagging. Although data are presented in this report as a function of parasitic load, load changes were effected by adjusting the useful load bank, thereby forcing compensation by the parasitic load.

The instrumentation used is true rms responding over a wide frequency range.

Specifications are detailed in appendix B. Included by each piece of equipment listed is a note as to which parameters each was used to measure. Power measurements were made with the aid of current transformers as were the current measurements, which also required precision shunts. The shunt outputs and the line-to-neutral voltages were connected to a true rms to dc converter. The converter output was then read on a digital voltmeter. Wattmeter outputs were read directly on the digital voltmeter. Periodically during the testing, instrument calibration was checked against a 0.25-percent voltage standard. A more detailed description of the overall test apparatus used to obtain the data presented herein is found in reference 12.

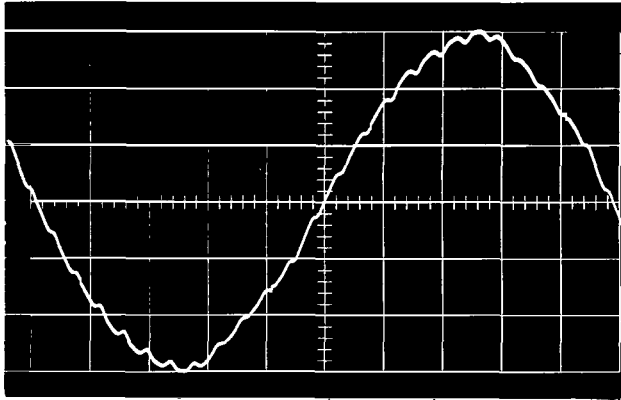
The methods used to obtain much of the experimental data are fairly straightforward. Of particular interest, however, is the equipment used for measuring the total harmonic distortion. A wide band current transformer is used for currents having an instantaneous output voltage equivalent to the waveshape of the current being measured. This output and the line-to-neutral voltage at the useful load are connected to a distortion analyzer through switch SW in figure 4. This analyzer is a high pass filter with a readout. The fundamental component of the signal is filtered out and the true rms value of the remaining harmonics is compared to the original signal and read on a meter. This reading is the rms value of the harmonics as a percent of the total signal.

RESULTS AND DISCUSSION

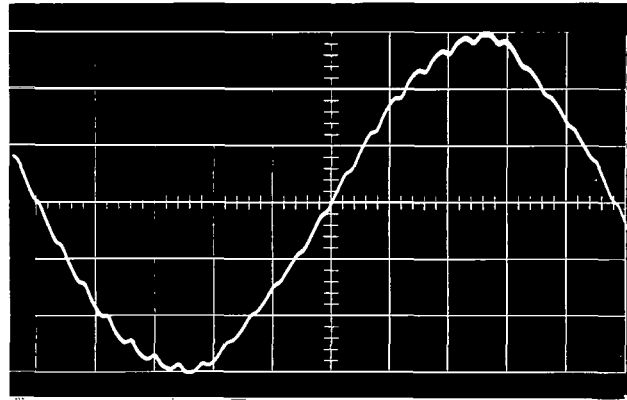
The variations of alternator output distortion and volt-ampere loading are each functions of parasitic load and the firing angle α for a given setting of the parasitic load bank. In order to keep the results as general as possible, the measured values of parasitic power are put into a per unit system. For all theoretical cases, 1 per unit parasitic load corresponds to 180° conduction per half cycle for each switching device in each parasitic load. Because of circuit limitations, this condition cannot be attained in a real system. Equivalent comparison of theoretical and experimental results thus requires a determination of experimental values which satisfy the definition of 1 per unit. This is accomplished by extrapolation of the maximum parasitic power measured to what it would be for 180° conduction. Raw data can then be normalized to this extrapolated value, thereby yielding experimental equivalents of theoretical per unit quantities. Equations used for this extrapolation are derived in appendix C.

Waveform Analysis

The analysis of harmonic distortion and volt-ampere loading in real parasitically loaded turboalternator systems is best started with a qualitative discussion of voltage



(a) Voltage. Total harmonic distortion, 3.30 percent.



(b) Current. Total harmonic distortion, 2.85 percent.

Figure 5. - Alternator waveforms for 9-kilowatt linear load. Lagging power factor, 0.97; parasitic load, 0.

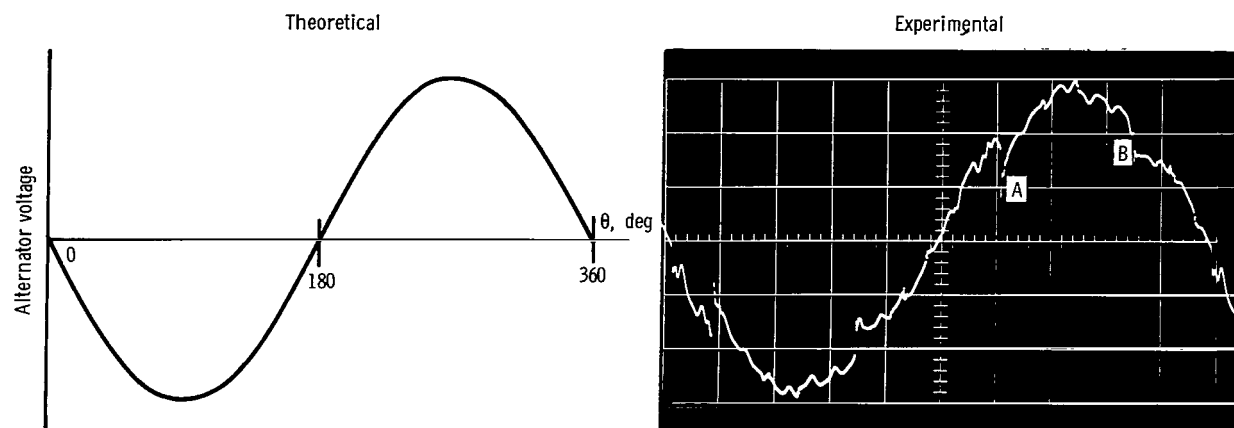
and current waveforms produced in such systems. At the same time, comparison of these experimental waveforms with those assumed for the analysis in reference 5 provides useful background information relevant to later discussions of quantitative data.

As stated previously, the theoretical power source produces a voltage free of harmonic distortion. In figure 5, waveforms and the total harmonic distortion (THD) are presented for the test alternator operating with a 9-kilowatt linear load. The distortion noted is produced entirely by the alternator. The ripple present in these waveforms is characteristic of small, high speed alternators.

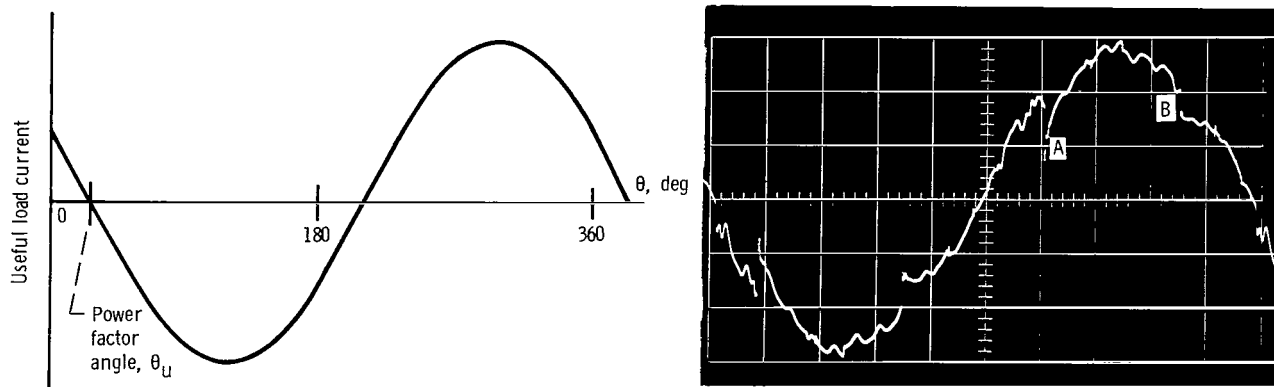
Figure 6 presents theoretical and experimental voltage and current waveforms for a typical turboalternator load configuration. Included are a useful load plus two parasitic loads, one turned fully on and one only partially on. The alternator terminal voltage is presented along with the following current components: the useful load current, the current in a fully on parasitic load, the current in a partially conducting parasitic load, and the total alternator current. The total current generated by the alternator is the sum of the three load currents noted.

This figure shows a qualitative comparison between the ideal and experimental voltage and current waveforms produced in parasitically loaded turboalternator systems. In particular, the analysis of the individual current components points out existing discrepancies and their origins. With this comparison, the major operational differences between the ideal and experimental systems become properly defined. The configuration presented is only one of many possible combinations. It is, however, representative and provides all the information desired. None of the waveforms presented in figure 6 are calibrated, and the following discussion is strictly qualitative.

In figure 6(a), the theoretical alternator terminal voltage is presented and is sinusoidal with zero distortion. The experimental waveform, however, shows extensive dis-



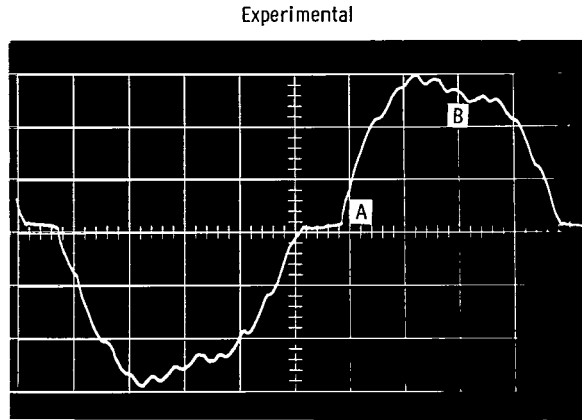
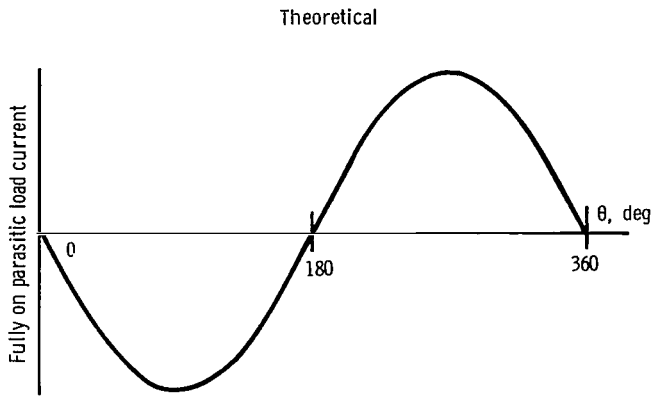
(a) Instantaneous alternator terminal voltage.



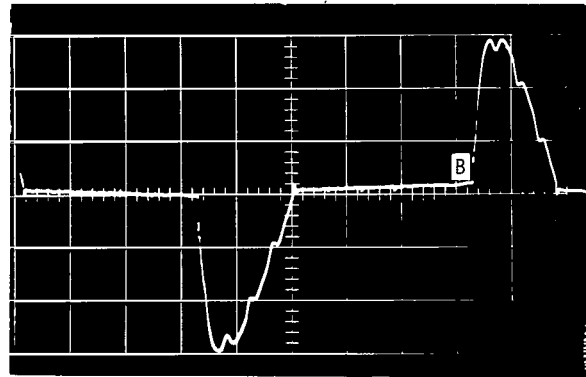
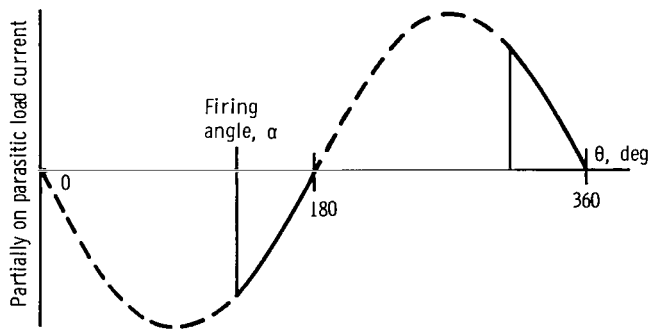
(b) Instantaneous useful load current.

Figure 6. - Comparison of typical voltage and current waveforms for turboalternator with useful load plus two phase-controlled parasitic loads. One parasitic load fully on and the other partially on.

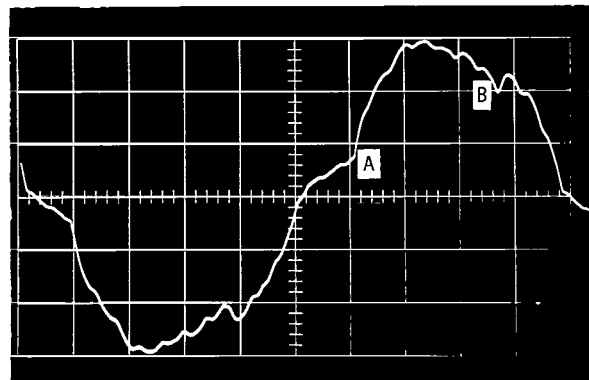
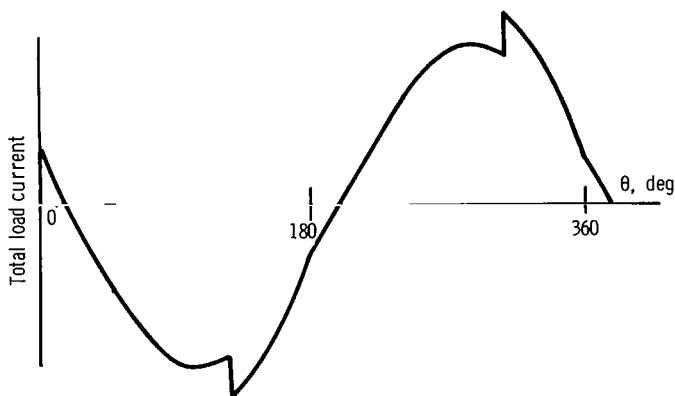
tortion. Part of this distortion is produced by the alternator itself as noted in figure 5. At points A and B in figure 6(a), severe notches appear which are the result of SCR's in the speed controller turning on. Note that these notches appear in each half cycle of the alternator output. When an SCR begins to conduct, a sudden rise in current occurs which increases the voltage drop across the internal impedance of the alternator, $R_A + X_A$, in figure 3. Since the voltage regulator cannot respond instantaneously to transients, the internally generated voltage E_G inside the machine remains constant, and the terminal voltage E_T drops almost instantaneously. This effect is the primary source of distortion in the voltage waveforms. The voltage waveform at the useful load is also very similar. It should be noted that the system tested did not include any provisions for filtering harmonic components of either the voltage or current.



(c) Instantaneous current of a fully on parasitic load.



(d) Instantaneous current of a partially on parasitic load.



(e) Instantaneous total generator current.

Figure 6. - Concluded.

The useful load current is presented in figure 6(b). The theoretical current is sinusoidal and is shifted with respect to the alternator terminal voltage by θ_u , the useful load power factor angle, which is an independent variable. The experimental current is shown for a value of θ_u very near zero (power factor very near unity) and is very similar to the alternator voltage waveform. This is expected because the useful load in this case is a linear resistive load. The experimental waveform in figure 6(b) points up the possibly undesirable effects of switching transients on the useful load output.

Instantaneous currents for a fully on parasitic load are shown in figure 6(c). In the theoretical case, the switching devices are assumed capable of conducting for a full 180° per half cycle. The result is a sinusoidal current with zero distortion. The experimental case points up the fact that, because of phase shifts in the parasitic control circuitry, the maximum attainable conduction interval is much less than 180° (see ref. 10). For the speed controller tested, maximum conduction varied from 140° to 160° per half cycle depending on the individual circuits. Note that points A and B correspond to those noted in part (a) of this figure. The depression in the current at point B results from the notch in the voltage due to the SCR firing in the second parasitic load. It is, of course, possible to have more than one parasitic load in a state of maximum conduction at a time. Again the configuration being discussed is simply a typical case.

Figure 6(d) shows instantaneous current for a partially on parasitic load. For the ideal case, a zero rise time is assumed. Once again this condition is not realized in the experimental case. The rise of current is actually more like an exponential. This is caused by test circuit reactances which, because they are inductive, tend to filter out the higher frequency current harmonics. Stated another way, there exists a time constant L/R which prevents instantaneous step changes in current from occurring. Again note that point B corresponds to the same points as in parts 6(a), (b), and (c).

Figure 6(e) shows the total alternator current, which is the sum of the useful load current, the fully on parasitic load current, and the partially on parasitic current. Most of the differences existing between the experimental and theoretical waveforms have been explained in figures 6(a) to (d). Again points A and B correspond to like locations in the other parts of this figure. The peak at point B of the experimental waveform is much less noticeable than in the theoretical case because of the notch effect in the voltage waveform caused by the SCR switching transient. In addition, the inductive filtering of the phase-controlled current in the partially conducting parasitic load is apparent from the rounded appearance of this peak in the experimental waveform.

The total generator current is of particular interest for distortion analysis. Total harmonic distortion (THD) affects the true rms or effective value of the total current which, in turn, has a direct effect on the volt-ampere demand of the alternator. Total volt-amperes is simply the product of the true rms alternator voltage and current summed over the three phases. Thus, the total current is the subject of investigation for both the theoretical and experimental cases.

Current Distortion

The analysis of experimental results requires definition of quantities of interest in terms of empirical data. The definition used in reference 5 for total harmonic distortion is given by

$$\text{THD} = \frac{(I_T^2 - I_{T1}^2)^{1/2}}{I_{T1}} \quad 100 \text{ percent} \quad (1)$$

where I_T and I_{T1} are single phase true rms quantities. As noted in the apparatus section of this report, the experimental testing yields results according to

$$\text{THD} = \frac{(I_T^2 - I_{T1}^2)^{1/2}}{I_T} \quad 100 \text{ percent} \quad (2)$$

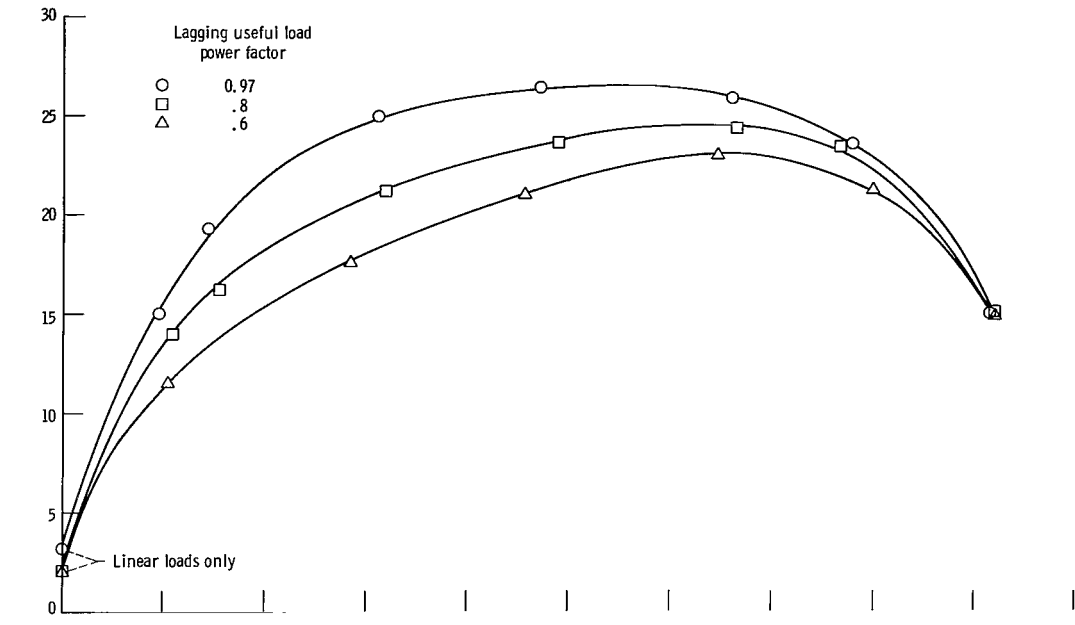
Analysis of this difference, however, shows that experimental values obtained according to equation (2) yield small errors relative to equation (1). For example, an experimental THD of 25 percent (which is close to the maximum value measured) corresponds to a value of 25.8 percent according to equation (1). This represents an error of about 3 percent which is acceptable for the analysis made.

Experimental and theoretical curves of alternator current distortion produced using one parasitic load are shown in figures 7(a) and (b), respectively. Useful load power factor is used as a parameter. The shapes of the two sets of curves are similar and both demonstrate a reduction in peak distortion with decreasing useful load power factor.

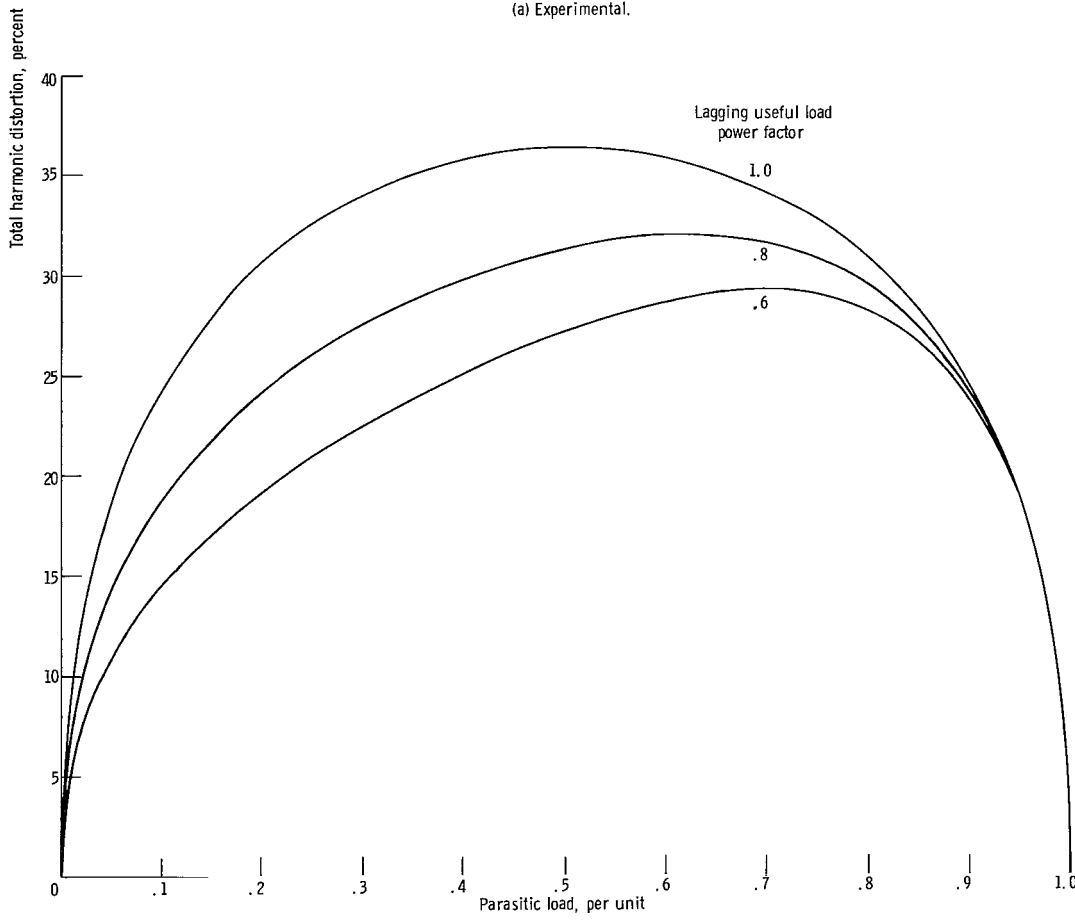
For the theoretical curves, zero distortion is attained at zero and 1 per unit parasitic load. This is expected because at zero parasitic load the alternator current equals useful load current and is, therefore, sinusoidal. In addition, the parasitic current at 1 per unit parasitic load (zero useful load) is a sinusoid.

In the experimental case, the distortion does not reduce to zero at zero parasitic load because of the residual harmonics generated by the alternator. These harmonic components are small relative to those produced by the parasitic loading. Therefore, alternator distortion probably has its greatest effect at this point. The experimental curves also do not extend to 1 per unit parasitic load. This results from the maximum conduction restrictions which occur in real systems. One per unit parasitic load for these curves is the extrapolated value corresponding to 180° conduction per half cycle for the SCR's.

The most significant difference between the experimental and theoretical results



(a) Experimental.



(b) Theoretical.

Figure 7. - Alternator current distortion for one parasitic load.

TABLE I. - MAXIMUM TOTAL
HARMONIC DISTORTION OF
ALTERNATOR CURRENT

(a) For single parasitic load

Useful load power factor (lagging)	Maximum distortion, percent	
	Experimental	Theoretical
1.0	--	37
.97	27	--
.8	25	32
.6	23	30

(b) For lagging useful load power factor, 0.8

Number of parasitic loads, N	Maximum distortion, percent	
	Experimental	Theoretical
1	25	32
2	15	18
3	16	13

lies in their relative magnitudes: the experimental values are significantly lower. This occurs despite the fact that the experimental alternator contributes to the distortion on its own. Table I(a) summarizes the peak harmonic distortion for the various useful load power factors. The differences noted result from the presence of inductive reactances in the experimental test circuit not considered in the theoretical analysis. The overall lowering of current distortion relative to the predictions of reference 5 will occur to some degree in any turboalternator electrical system having phase-controlled parasitic loading. The actual values obtained will depend, of course, on the hardware and the particular electrical circuit used.

The variation of current distortion with the number of parallel parasitic loads is presented in figures 8(a) and (b). The useful load power factor is 0.8 lagging. The experimental and theoretical cases differ at zero and 1 per unit parasitic load for the same reasons noted previously. In addition, the same general conclusion regarding lower experimental distortion can be made for the case of two parasitic loads. This is not always true for three parasitic loads. Table I(b) summarizes the results for peak distortion.

For a three parasitic load configuration, the peak experimental distortion of the alternator current is 3 percent higher than the theoretical value. This effect is caused

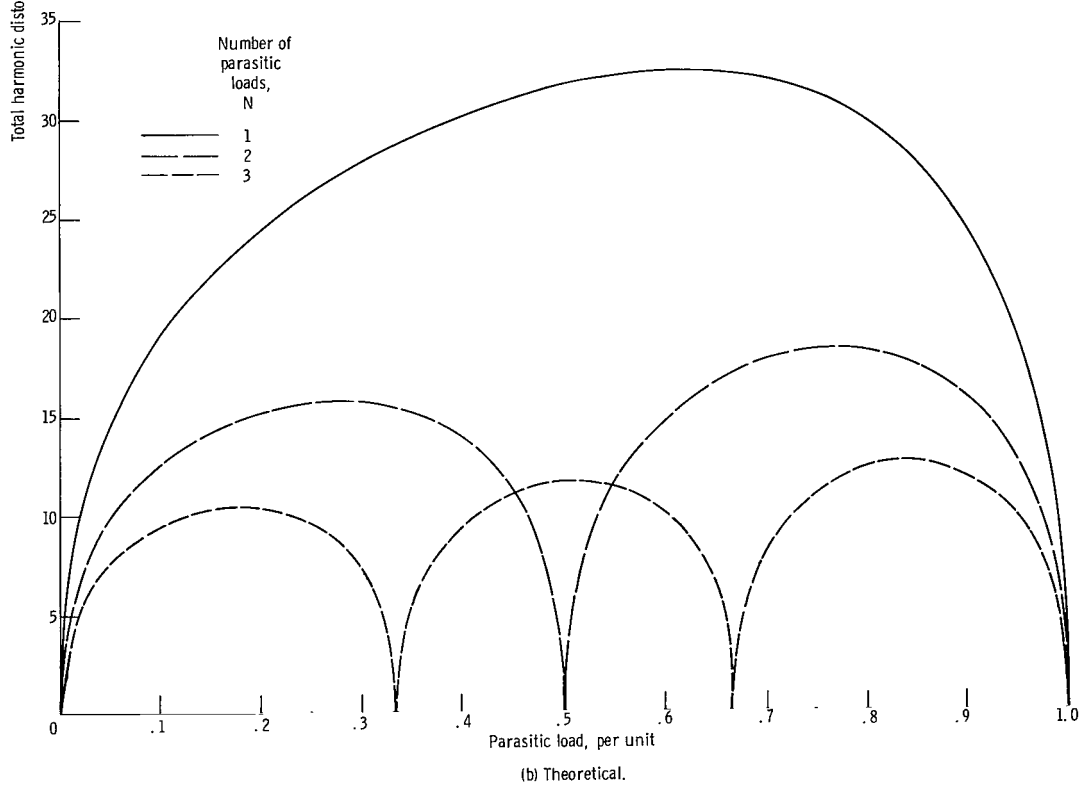
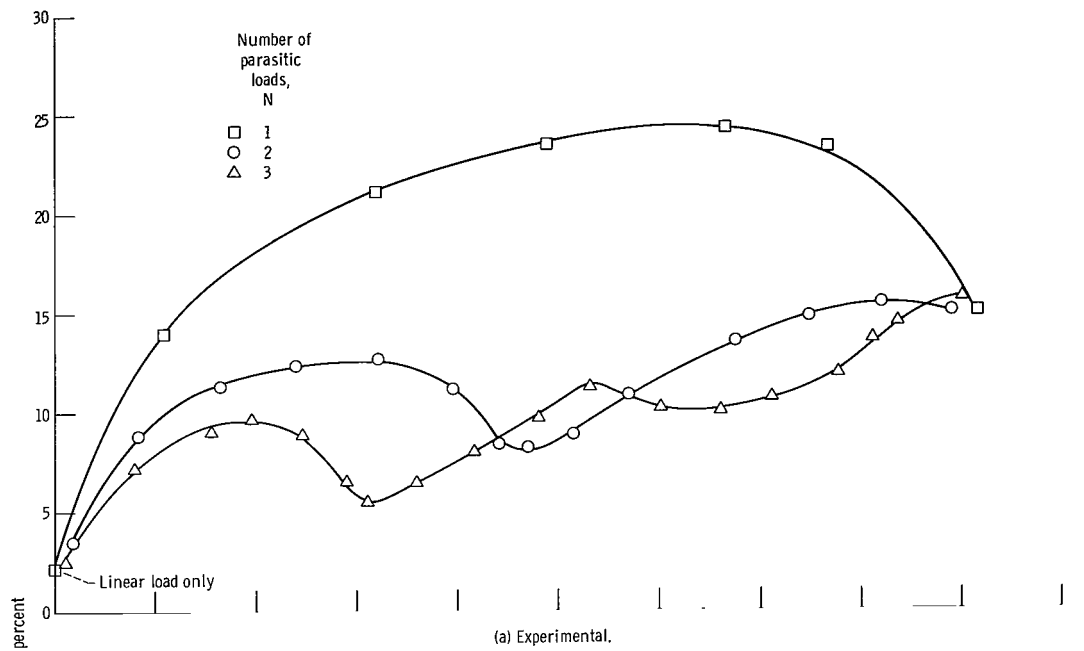


Figure 8. - Alternator current distortion for N parallel parasitic loads. Lagging useful load power factor, 0.8.

by the overlap of parasitic load operating ranges and by the limited conduction interval of the SCR's in the test circuit. In figure 8(b), the theoretical distortion for two parasitic loads goes to zero at 0.5 per unit. Likewise, for three parasitic loads, the distortion is zero at 0.33 and 0.67 per unit load. This is expected because there is no overlap in the theoretical model and because the ideal switch is assumed capable of conducting for a full 180° per half cycle. The theoretical current in a fully on parasitic load is a sinusoid with zero distortion (see fig. 6(c)).

In the experimental case, the limited conduction range has a cumulative effect on the value of harmonic distortion. For the two load experimental case in figure 8(a), the minimum distortion at 0.47 per unit (one load fully on) is very nearly half the distortion for the maximum load at 0.89 per unit (two loads fully on). In the same way for the three load case, the minimums at 0.31 per unit (one load fully on) and at 0.63 per unit (two loads fully on) are about one-third and two-thirds, respectively, of the maximum distortion occurring at 0.9 per unit (three loads fully on). When slight differences in maximum conduction intervals are disregarded between parasitic loads, each fully on parasitic load introduces a "residual" distortion. This residual distortion cannot be reduced by further action of additional parasitic loads. At approximately 0.9 per unit parasitic load, each experimental combination of loads is at maximum conduction. The distortion is virtually the same in each case with slight variations probably due to instrumentation errors. Therefore, there exists a limit as to the extent to which maximum distortion of the alternator current can be reduced by increasing the number of parasitic loads. As a result, the effect of increasing the number of parasitic loads in order to reduce the overall harmonic distortion also becomes limited. This limitation results from the inability of experimental parasitic loads to conduct for a full 180° per half cycle. However, if the maximum SCR conduction interval could be increased by modification of the phase control circuitry, this limitation could be minimized. In general, the greater the conduction interval, the more the overall distortion can be reduced by increasing the number of parasitic loads.

Voltage Distortion and Crest Factor

Closely related to the total harmonic distortion of the alternator current are the distortion and crest factor of the voltage at the useful load. The variation of both of these with parasitic loading is of interest because they reflect the quality of the useful system output.

Figure 9 presents useful load voltage distortion for one parasitic load. A substantial increase occurs in this distortion over the value indicated for a linear load at zero parasitic load (1 per unit useful load). Most of the distortion is due to the notching ef-

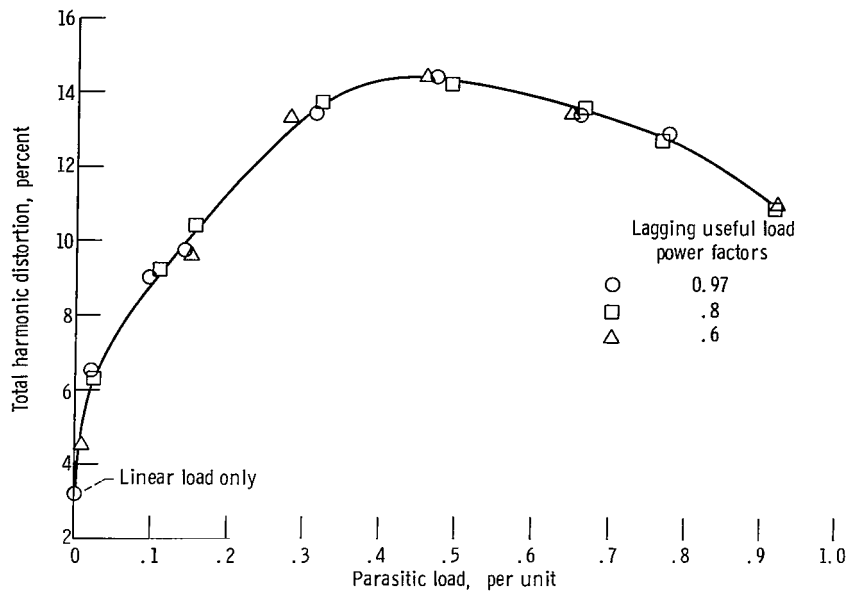


Figure 9. - Useful load voltage distortion for one parasitic load.

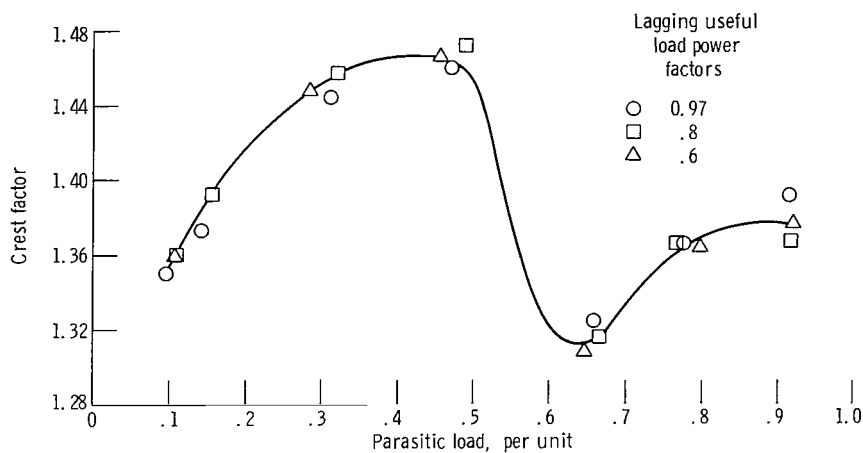


Figure 10. - Useful load voltage crest factor for one parasitic load.

fect in the alternator voltage resulting from SCR turn-on transients. Note also that unlike the current harmonics, the voltage distortion is independent of useful load power factor. This high level of distortion also occurs in the useful load current (although the current distortion varies with useful load power factor) and could prove unacceptable for certain loads where high frequency voltage and current components are undesirable.

A second means of evaluating the effects of the speed controller on the useful load is the crest factor, shown in figure 10 for one parasitic load. Crest factor is defined as the ratio of the peak voltage to the true rms voltage and equals $\sqrt{2}$ for a sine wave. The actual value of the crest factor in the experimental curves is not so much of interest as is the variation of this value over the operating range of one speed control section. The maximum value on the curve is almost 1.47, and the minimum is 1.31. This variation

results from the changing SCR firing angle α . As noted earlier, at the point in the voltage waveform where SCR turn-on occurs, a notch appears which is an instantaneous drop in the alternator voltage. This phenomenon results from the increased voltage drop across the alternator impedance. When this notching takes place just before the point $\alpha = 90^\circ$, the peak voltage is significantly reduced. The result is an abrupt change in the crest factor.

The crest factor is important for voltage regulation. Many voltage regulator sensing circuits, including the unit tested, are sensitive to wide variations in crest factor in trying to regulate the true rms voltage. The result is that the voltage regulation of the alternator regulator with parasitic loading is not as good as with linear loads only. This fact is pointed out here because it is related to the problem of harmonic distortion resulting from nonsinusoidal currents. Further examination of regulation characteristics is beyond the scope of this report, however.

Volt-Ampere Requirements

Alternator volt-ampere loading is presented in terms of normalized and relative volt-amperes. Because the speed controller tested exhibited unbalanced loads and voltages between phases, three phase quantities are necessarily analyzed.

Alternator normalized volt-amperes (NVA) defined as the ratio of the total alternator volt-amperes to the total alternator power is given by

$$\text{NVA} = \frac{\sum_{\varphi=1}^3 E_{T\varphi} I_{\varphi}}{\sum_{\varphi=1}^3 P_{G\varphi}} \quad (3)$$

where $E_{T\varphi}$, I_{φ} , and $P_{G\varphi}$ are each experimentally measured, true rms quantities. The reciprocal of NVA is the alternator power factor. When NVA is plotted as a function of parasitic load, the maximum volt-ampere demand on the alternator is determined. In reference 5, $P_{G\varphi}$ is a constant (rated power) and the quantity NVA is termed per unit volt-amperes where 1 per unit equals rated power. For the purposes of this report, however, NVA is used for both theoretical and experimental data.

Relative volt-amperes (RVA) (termed relative apparent power in ref. 5) defined for a given useful load power factor $\cos \theta_u$ is

$$RVA = \frac{\text{Volt-amperes required with parasitic load}}{\text{Volt-amperes required without parasitic load}} \quad (4)$$

The denominator of equation (4) represents the condition wherein a linear load only is applied to the alternator. Alternator volt-amperes for this condition are given by

$$VA_{\text{linear load}} = \sum_{\varphi=1}^3 \frac{P_{G\varphi}}{\cos \theta_u} \quad (5)$$

Again $P_{G\varphi}$ is a measured quantity which remains essentially constant. The useful load power factor $\cos \theta_u$ is treated as a constant for this calculation. The numerator of equation (4) is equivalent to the numerator of equation (3). Thus, in terms of experimentally measured quantities, equation (4) becomes

$$RVA = \frac{\sum_{\varphi=1}^3 E_{T\varphi} I_{\varphi}}{\sum_{\varphi=1}^3 \frac{P_{G\varphi}}{\cos \theta_u}} \quad (6)$$

When RVA is plotted as a function of parasitic load, the maximum increase in alternator volt-ampere capacity necessitated by the phase-controlled parasitic load is determined. Again for NVA and RVA, the number of parasitic loads and the useful load power factor are independent variables.

In the ideal case, phase-controlled loading of a turboalternator increases the volt-ampere requirements in two ways. First, the current components at harmonic frequencies, having no equivalent counterparts in the ideal voltage waveform, do not dissipate power while they do increase the effective value of the current. Secondly, the fundamental component of the phase-controlled current generally lags the applied voltage. Therefore, lagging power factor also increases the volt-ampere needs. Because the experimental current distortion is significantly lower than predicted, the volt-ampere requirements might also be expected to be lower. This is not the case as shown in figure 11. This figure presents normalized alternator volt-ampere loading as a function of parasitic load for one speed control section. The peak values, which are shown in table II, indicate only slight variations between the experimental and ideal cases. This result is largely due to the inductive reactances which attenuate the current harmonics.

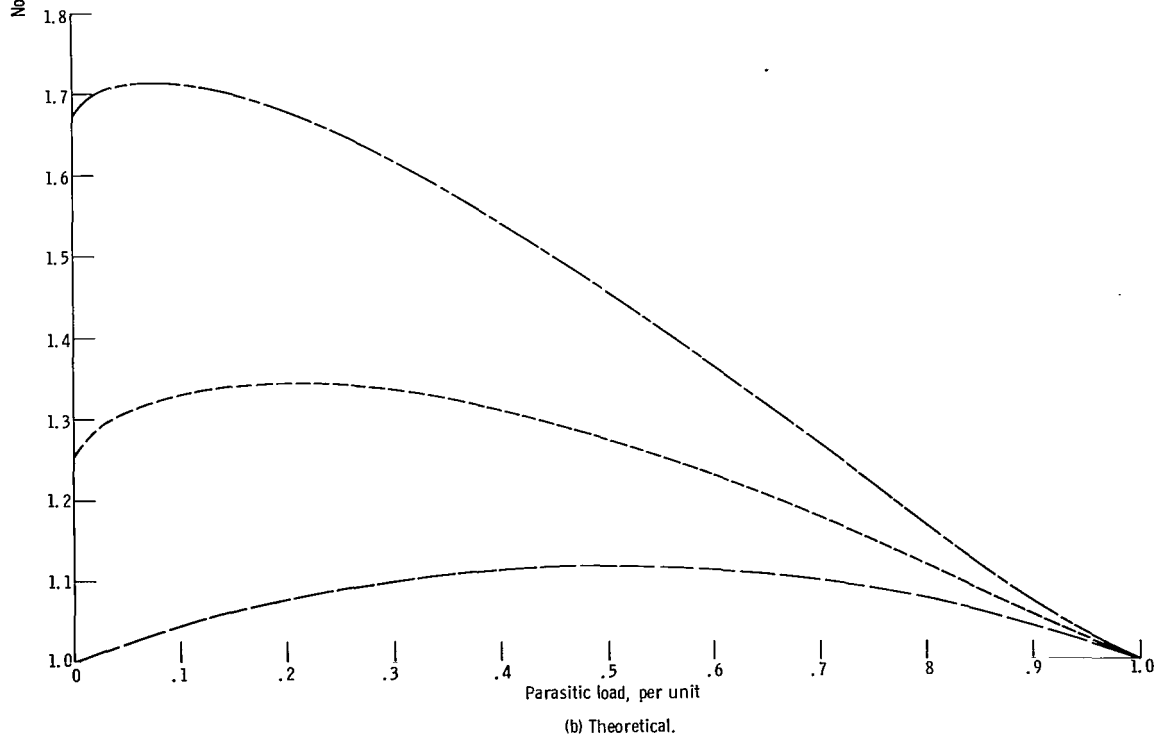
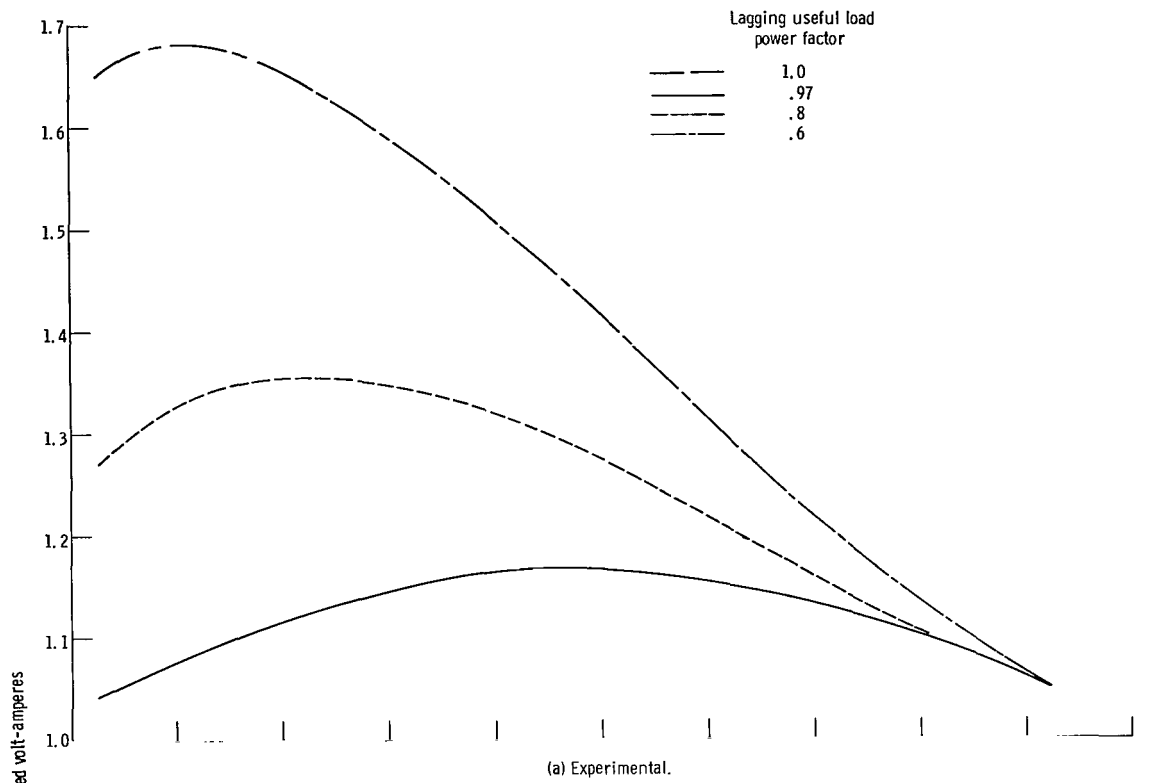


Figure 11. - Alternator volt-amperes normalized to alternator power for one parasitic load.

TABLE II. - PEAK VOLT-AMPERES^a REQUIRED OF
ALTERNATOR WITH LINEAR LOAD PLUS
ONE PARASITIC LOAD

Useful load power factor (lagging)	Linear load only (theoretical)	Linear load plus parasitic load	
		Experimental	Theoretical
1.0	1.00	----	1.12
.97	1.03	1.17	----
.8	1.25	1.36	1.35
.6	1.67	1.68	1.72

^aNormalized to total alternator power.

The presence of these reactances introduces additional voltage drops in the test circuit. As a result the alternator terminal voltage must increase to provide the necessary power to the loads. Consequently, little change is observed in the volt-ampere products of equation (3). Note that the peak values of the experimental curves are a measure of the minimum capacity for which the alternator must be rated in order to operate in this configuration. For example, operating at rated power with a 0.8 lagging useful load power factor and one parasitic load, the alternator must have a volt-ampere capacity equal to or greater than 1.36 times its total output power. The peak value increases with decreasing useful load power factor simply because the reactive loading of a linear load increases as the power factor becomes less.

Figure 12 shows the alternator volt-amperes required when using a single parasitic load relative to the volt-amperes required without the parasitic load. For the cases both with and without the parasitic load, the total alternator power is the same and the useful load power factor is the same. This ratio (RVA) is a measure of the necessary increase in alternator volt-ampere rating required when using phase-controlled parasitic loads rather than linear parasitic loads. For example, consider the case of 0.8 lagging useful load power factor. As noted earlier, the peak volt-ampere demand is 1.36 times the power output as shown in figure 11(a). For a linear load at 0.8 power factor, the volt-ampere requirement is 1.25 times the real power. Thus, the ratio of peak volt-amperes required using the parasitic load relative to the alternator volt-amperes without the parasitic load (in this case a linear 0.8 power factor load) is simply $1.36/1.25$ or 1.08. A value of RVA greater than one indicates that the volt-ampere demand occurring with the parasitic loading is greater than that for an equal but linear load. Note that the volt-amperes of the linear load is determined on the basis of total alternator power and the useful load power factor designated for each of the individual curves in figure 12.

Peak values are tabulated in table III(a) and the correlation between experimental and

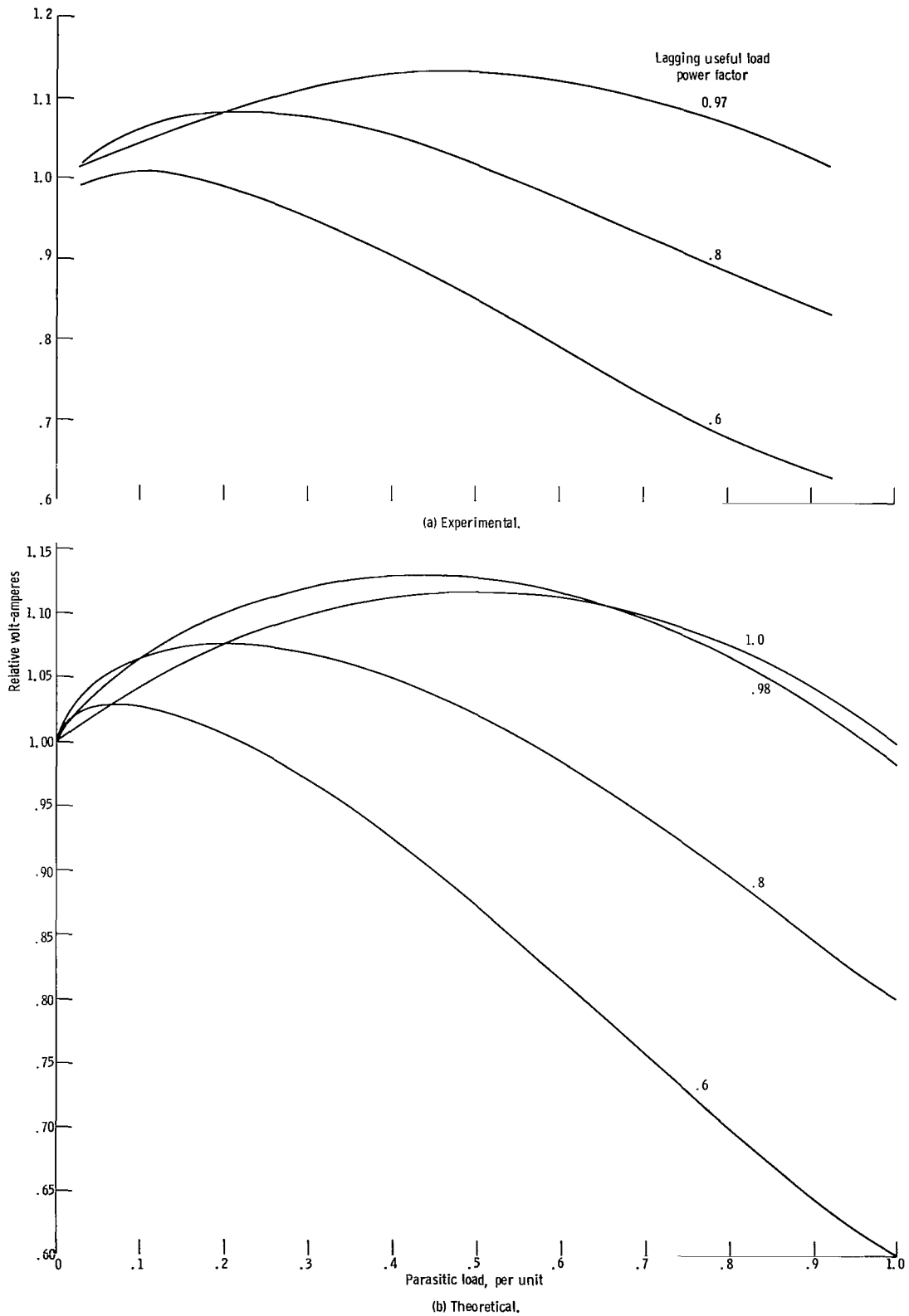


Figure 12. - Alternator volt-amperes using one parasitic load relative to volt-amperes required without parasitic load.

TABLE III. - PEAK VOLT-AMPERES
 REQUIRED OF ALTERNATOR WITH
 PARASITIC LOAD RELATIVE TO
 ALTERNATOR VOLT-AMPERES
 REQUIRED WITHOUT
 PARASITIC LOAD

$$\left[\text{Relative volt-amperes} = \frac{\text{Volt-amperes required with parasitic load}}{\text{Volt-amperes required without parasitic load}} \right]$$

(a) For one parasitic load

Useful load power factor (lagging)	Peak volt-amperes required	
	Experimental results	Theoretical results
1.0	-----	1.12
.984	-----	^a 1.131
.97	1.135	-----
.96	-----	1.10
.8	1.08	1.08
.6	1.01	1.03

(b) For lagging useful load power factor, 0.8

Number of parasitic loads, N	Peak volt-amperes required	
	Experimental results	Theoretical results
1	1.08	1.08
2	1.03	1.03
3	1.02	1.02

^aPeak theoretical value.

theoretical results is quite good. It is interesting to note that the 0.6 power factor curve in figure 12(a) drops below one for per unit values of parasitic load below 0.05. This results from the effect that the speed controller shutoff losses have an overall parasitic loading. For the speed controller tested, these losses occur at a lagging power factor greater than 0.9. For small enough parasitic loads, these losses have a dominant effect; and the parasitic load actually operates at a higher power factor than the useful load.

The variation of relative volt-amperes for one, two, and three parasitic loads at 0.8 lagging useful load power factor is shown in figure 13. The peak values summarized in table III(b) show excellent correlation. The actual difference between the two sets of results is, in each case, less than 1 percent. The reduction in volt-amperes with increasing number of parasitic loads is quite obvious from these curves.

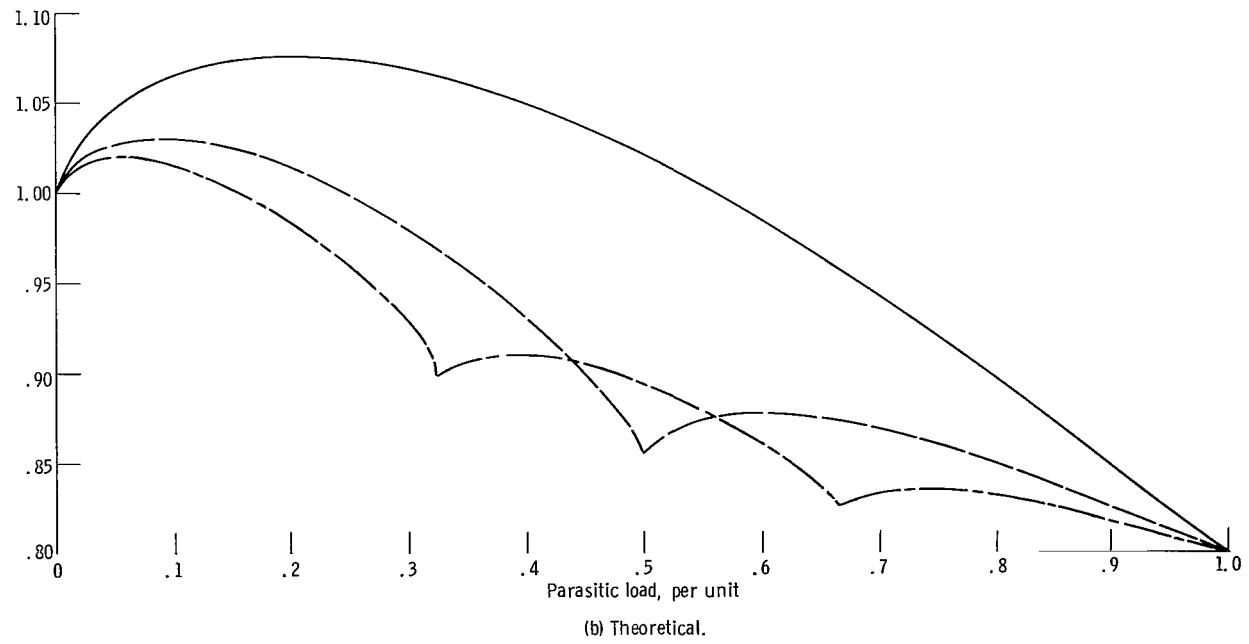
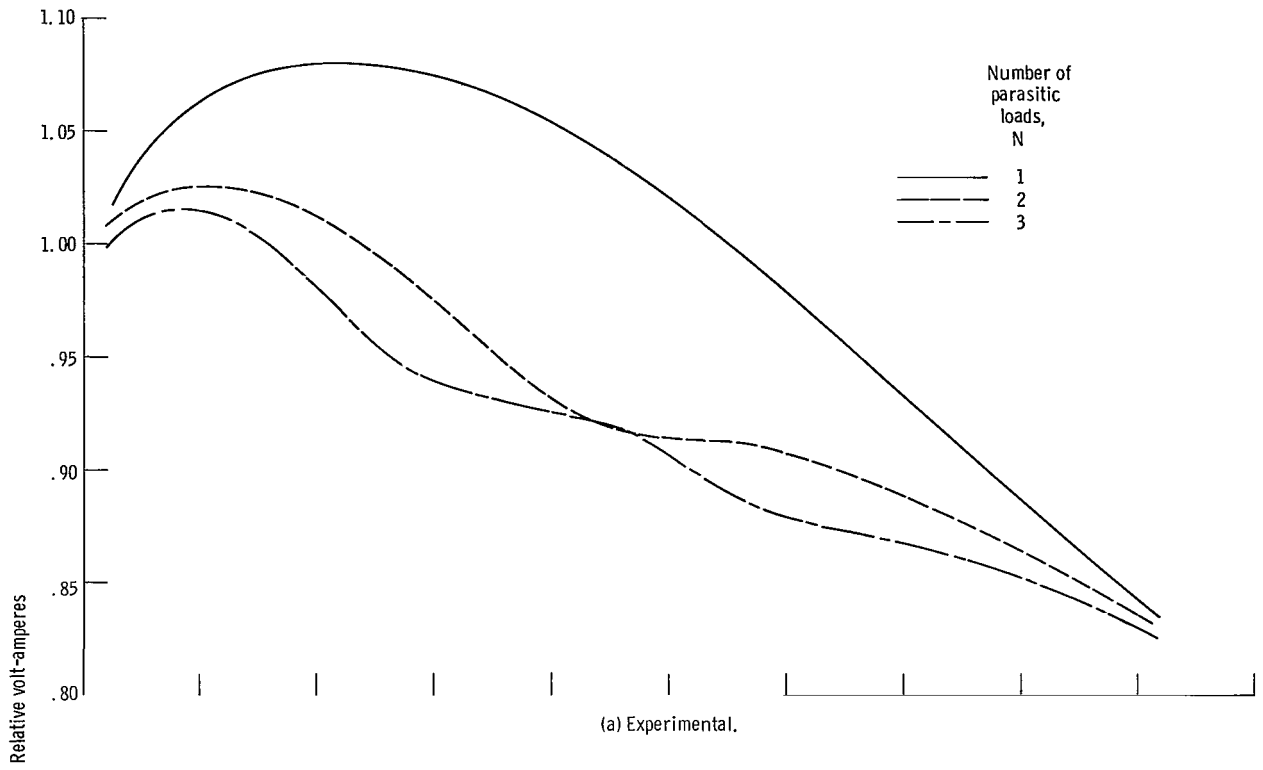


Figure 13. - Alternator volt-amperes required with N parallel parasitic loads relative to alternator volt-amperes without parasitic loads. Lagging useful load power factor, 0.8.

It should be noted that the degree of correlation between the experimental and theoretical results for normalized volt-amperes and relative volt-amperes is probably due in part to offsetting differences between real and ideal systems. There are many important differences which exist, and these have been noted in earlier sections of this report. It is significant that there is good correlation between theoretical predictions and experimental results despite these differences. In addition, similar results may be expected from other experimental systems of this type.

SUMMARY OF RESULTS

The variation of alternator volt-ampere loading and output harmonic distortion was experimentally determined for several parasitic loading conditions. The number of parasitic loads and the useful load power factor were used as parameters. The results were compared with theoretical data for the same conditions. The following results were obtained:

1. The experimental current harmonics were significantly lower than the theoretical predictions. For a 0.8 lagging useful load power factor, the experimental peak current distortion was lower by 24 percent of the theoretical value using one parasitic load and by 16 percent using two loads. This difference was caused by inductive reactances in the test circuit which were not considered in the ideal case.

2. A limitation exists as to the extent to which current distortion can be reduced by increasing the number of parasitic loads. This limitation arises from restrictions in the maximum conduction interval attainable by real parasitic loads. In the system tested, a smaller than predicted decrease in overall distortion occurred between two and three parasitic loads with no decrease occurring in the peak value.

3. For 0.8 lagging useful load power factors, the alternator relative volt-amperes using one, two, and three parasitic loads was in each case within 1 percent of the theoretical value.

Lewis Research Center,
National Aeronautics and Space Administration,
Cleveland, Ohio, September 11, 1969,
120-27.

APPENDIX A

SYMBOLS

E_G	rms value of internally generated alternator voltage
E_T	rms value of alternator terminal voltage
$E_{T\varphi}$	E_T on phase φ , V
I_T	rms value of total alternator current
I_{T1}	rms value of fundamental component of total alternator current
$I_{T\varphi}$	I_T on phase φ , A
K	designation of individual parasitic load $K = 1, 2, \dots, N$
N	total number of parasitic loads
NVA	normalized volt-amperes
$P_{G\varphi}$	rms value of alternator power on phase φ , W
$P_{P\varphi}$	rms value of parasitic power on phase φ , W
$(P_{P\varphi})_1$ per unit	extrapolated value of $P_{P\varphi}$ corresponding to 180° conduction per half cycle for experimental data, W
$(P_P)_1$ per unit	$(P_{P\varphi})_1$ summed over three phases, W
R_A	effective internal alternator resistance
R_E	series resistance of static exciter
R_{PK}	effective parasitic load resistance on load K
R_R	effective parallel resistance of voltage regulator
R_{SCL}	effective resistance of parasitic load control circuitry
R_U	effective useful load resistance
RVA	relative volt-amperes
THD	total harmonic distortion, percent
$V_{P\varphi}$	rms value of input voltage on phase φ of the speed controller, V
$V_{P\varphi K}$	rms value of voltage across resistor R_{PK} on phase φ , V
X_A	effective internal reactance of alternator
X_E	series reactance of static exciter

X_{LPK} equivalent reactance of parasitic load K produced by phase-controlled current
 X_R effective parallel reactance of voltage regulator
 X_{RPK} effective reactance of parasitic load bank K autotransformer
 X_{RU} effective reactance of useful load bank autotransformer
 X_{SCL} effective reactance of parasitic load control circuitry
 α firing angle of phase-controlled current
 θ_u useful load power factor angle

APPENDIX B

INSTRUMENT SPECIFICATIONS

The following are the instruments used for measuring the data presented in this report. The parameters measured by each piece of equipment are noted in parenthesis.

True rms to dc converter (voltage and current):

Input voltage: 9×10^{-3} to 1×10^3 V rms

Accuracy: 0.1 percent of full-scale deflection (20° to 30° C)

Frequency response: 40 to 3×10^4 Hz

Input impedance: $1 \text{ M}\Omega \pm 0.05$ percent paralleled with 60 to 80 pf depending on input range

Output full-scale voltage: 3 or 10 V dc depending on input range

Integrating digital voltmeter (voltage, current, and power):

Input voltage: 0 to 1000 V dc

Accuracy: 0.01 percent ± 1 digit

Input impedance: 1×10^5 to 1×10^7 Ω depending on range

Precision shunt (current):

Resistance: 0.1 Ω

Capacity: 15 A

Accuracy: 0.04 percent (in air)

Current transformer (current and power):

Current ratio: 50/5 A

Ratio error: ± 0.1 percent (70 to 2500 Hz)

Capacity: 25 V-A

Wattmeter (power):

Input voltage: 50, 100, and 200 V (nominal)

Input current: 5 A (nominal)

Accuracy (output): 0.1 percent

Frequency range: dc to 2500 Hz

Current transformer (current distortion):

Input current: 50 A rms

Output voltage: 0.1 V/A

Frequency response: down 3 dB at 1 and 3.5×10^7 Hz

Distortion analyzer (voltage and current distortion):

Measurement range: any fundamental, 5 to 6×10^5 Hz

Elimination characteristics: fundamental rejection > 80 dB

Accuracy: ± 3 percent

True rms voltmeter (voltage and current distortion):

Voltage range: 1×10^{-3} to 300 V rms

Accuracy: 1 percent of full-scale deflection

Frequency range: 50 to 1×10^6 Hz

Peak voltmeter (crest factor):

Voltage range: 3×10^{-4} to 330 V

Accuracy: 3 percent of full-scale deflection

Frequency range: 20 to 4×10^5 Hz

APPENDIX C

CALCULATION OF 1 PER UNIT PARASITIC LOAD VALUES FROM EXPERIMENTAL DATA

The measurement locations of experimental data used to calculate 1 per unit parasitic power are shown schematically in figure 14 for one phase φ ($\varphi = 1, 2, 3$) and one load K ($K = 1, 2, \dots, N$) of a three-phase speed controller with N parallel parasitic loads. The line-to-neutral voltages with units of volts are $V_{P\varphi}$ and $V_{P\varphi K}$. The power with units of watts is $P_{P\varphi}$. Control circuitry losses and voltage drops across the SCR's are not considered because they are quite small.

On a given phase, the maximum attainable rms voltage $(V_{P\varphi K})_{MAX}$ across each

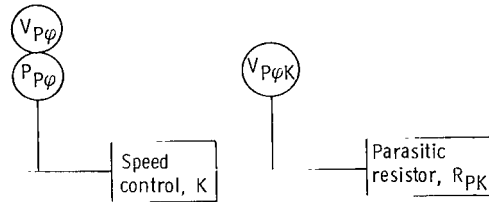


Figure 14. - Schematic diagram showing instrumentation on phase φ and parasitic load K of N parallel three phase parasitic loads.

parasitic resistor can vary substantially from load to load because of variations in maximum SCR conduction. Therefore, the maximum total power dissipated in one phase of N parallel parasitic loads at maximum attainable conduction is given by

$$(P_{P\varphi})_{MAX} = \sum_{K=1}^N \frac{(V_{P\varphi K})_{MAX}^2}{R_{PK}} \quad (C1)$$

where R_{PK} is the parasitic resistance in ohms. For 180° conduction per half cycle on each parasitic load, $V_{P\varphi} = V_{P\varphi K}$ for all K (neglecting voltage drops across the SCR's). The experimental 1 per unit value, based on 180° conduction per half cycle for each SCR, is, therefore,

$$(\text{P}_{\text{P}\varphi})_{1 \text{ per unit}} = V_{\text{P}\varphi}^2 \sum_{\text{K}=1}^{\text{N}} \frac{1}{\text{R}_{\text{PK}}} \quad (\text{C2})$$

Since all R_{PK} are adjusted to be equal, equation (C1) then becomes

$$(\text{P}_{\text{P}\varphi})_{\text{MAX}} = \frac{1}{\text{R}_{\text{P}}} \sum_{\text{K}=1}^{\text{N}} (V_{\text{P}\varphi\text{K}})_{\text{MAX}}^2 \quad (\text{C3})$$

Equation (C2) becomes

$$(\text{P}_{\text{P}\varphi})_{1 \text{ per unit}} = V_{\text{P}\varphi}^2 \frac{\text{N}}{\text{R}_{\text{P}}} \quad (\text{C4})$$

Dividing equation (C3) by equation (C4) and solving for $(\text{P}_{\text{P}\varphi})_{1 \text{ per unit}}$ yields

$$(\text{P}_{\text{P}\varphi})_{1 \text{ per unit}} = \frac{(\text{P}_{\text{P}\varphi})_{\text{MAX}} \text{N} V_{\text{P}\varphi}^2}{\sum_{\text{K}=1}^{\text{N}} (V_{\text{P}\varphi\text{K}})_{\text{MAX}}^2} \quad (\text{C5})$$

For the three phase case

$$(\text{P}_{\text{P}})_{1 \text{ per unit}} = \text{N} \sum_{\varphi=1}^3 \frac{(\text{P}_{\text{P}\varphi})_{\text{MAX}} V_{\text{P}\varphi}^2}{\sum_{\text{K}=1}^{\text{N}} (V_{\text{P}\varphi\text{K}})_{\text{MAX}}^2} \quad (\text{C6})$$

$(\text{P}_{\text{P}})_{1 \text{ per unit}}$ has units of watts and is evaluated entirely from experimental data.

REFERENCES

1. Bernatowicz, Daniel T.: NASA Solar Brayton Cycle Studies. Paper presented at the Symposium on Solar Dynamic Systems Sponsored by Solar and Mechanical Working Groups of the Interagency Advanced Power Group, Washington, D. C., Sept. 24-25, 1963.
2. Klann, John L.: 2 to 10 Kilowatt Solar or Radioisotope Brayton Power System. Intersociety Energy Conversion Engineering Conference. Vol. I. IEEE, 1968, pp. 407-415.
3. Repas, David S.; and Valgora, Martin E.: Voltage Distortion Effects of SNAP-8 Alternator Speed Controller and Alternator Performance Results. NASA TN D-4037, 1967.
4. Dauterman, W. E.; and Viton, E. J.: SNAP-II Rotational Speed Control. IRE Trans. Nucl. Sci., vol. NS-9, Jan. 1962, pp. 151-157.
5. Gilbert, Leonard J.: Reduction of Apparent-Power Requirement of Phase-Controlled Parasitically Loaded Turboalternator by Multiple Parasitic Loads. NASA TN D-4302, 1968.
6. Corcoran, Charles S.; and Yeager, LeRoy J.: Summary of Electrical Component Development for a 400-Hertz Brayton Energy Conversion System. NASA TN D-4874, 1968.
7. Dryer, A. M.; Kirkpatrick, F. M.; Russell, E. F.; Himsatt, J. M.; and Yeager, L. J.: Alternator and Voltage Regulator-Exciter Design and Development. Vol. 1. General Electric Co., June 9, 1967. (Contract number NAS3-6013.)
8. Edkin, Richard A.; Valgora, Martin E.; and Perz, Dennis A.: Performance Characteristics of 15 kVA Homopolar Inductor Alternator for 400 Hz Brayton-Cycle Space-Power System. NASA TN D-4698, 1968.
9. Bollenbacher, Gary; Edkin, Richard A.; and Perz, Dennis A.: Experimental Evaluation of a Voltage Regulator-Exciter for a 15 Kilovolt-Ampere Brayton Cycle Alternator. NASA TN D-4697, 1968.
10. Word, John L.; Fischer, Raymond L. E.; and Ingle, Bill D.: Static Parasitic Speed Controller for Brayton-Cycle Turboalternator. NASA TN D-4176, 1967.
11. Fischer, Raymond L. E.; and Droba, Darryl J.: Dynamic Characteristics of Parasitic-Loading Speed Controller for 10-Kilowatt Brayton Cycle Turboalternator. NASA TM X-1456, 1968.
12. Wood, James C.; Valgora, Martin E.; Kruchowy, Roman; Curreri, Joseph S.; Perz, Dennis A.; and Tryon, Henry B.: Preliminary Performance Characteristics of a Gas-Bearing Turboalternator. NASA TM X-1820, 1969.

FIRST CLASS MAIL



POSTAGE AND FEES PAID
NATIONAL AERONAUTICS
SPACE ADMINISTRATION

04L 001 2P 51 3DS 69345 00903
AIR FORCE WEAPONS LABORATORY/WL117
KIRTLAND AIR FORCE BASE, NEW MEXICO 87117

ATTN: LEO BOWMAN, CHIEF, TECH. LIBRARY

POSTMASTER: If Undeliverable (Section 1
Postal Manual) Do Not Re

"The aeronautical and space activities of the United States shall be conducted so as to contribute . . . to the expansion of human knowledge of phenomena in the atmosphere and space. The Administration shall provide for the widest practicable and appropriate dissemination of information concerning its activities and the results thereof."

— NATIONAL AERONAUTICS AND SPACE ACT OF 1958

NASA SCIENTIFIC AND TECHNICAL PUBLICATIONS

TECHNICAL REPORTS: Scientific and technical information considered important, complete, and a lasting contribution to existing knowledge.

TECHNICAL NOTES: Information less broad in scope but nevertheless of importance as a contribution to existing knowledge.

TECHNICAL MEMORANDUMS: Information receiving limited distribution because of preliminary data, security classification, or other reasons.

CONTRACTOR REPORTS: Scientific and technical information generated under a NASA contract or grant and considered an important contribution to existing knowledge.

TECHNICAL TRANSLATIONS: Information published in a foreign language considered to merit NASA distribution in English.

SPECIAL PUBLICATIONS: Information derived from or of value to NASA activities. Publications include conference proceedings, monographs, data compilations, handbooks, sourcebooks, and special bibliographies.

TECHNOLOGY UTILIZATION PUBLICATIONS: Information on technology used by NASA that may be of particular interest in commercial and other non-aerospace applications. Publications include Tech Briefs, Technology Utilization Reports and Notes, and Technology Surveys.

Details on the availability of these publications may be obtained from:

SCIENTIFIC AND TECHNICAL INFORMATION DIVISION
NATIONAL AERONAUTICS AND SPACE ADMINISTRATION
Washington, D.C. 20546